Rearrangements between differentiating hair cells coordinate planar polarity and the establishment of mirror symmetry in lateral-line neuromasts

Ivana Mirkovic, Serhiy Pylawka and A. J. Hudspeth*

Howard Hughes Medical Institute and Laboratory of Sensory Neuroscience, The Rockefeller University, 1230 York Avenue, New York, NY 10065, USA

*Author for correspondence (hudspaj@rockefeller.edu)

Biology Open 1, 498–505
doi: 10.1242/bio.2012570

Summary

In addition to their ubiquitous apical-basal polarity, many epithelia are also polarized along an orthogonal axis, a phenomenon termed planar cell polarity (PCP). In the mammalian inner ear and the zebrafish lateral line, PCP is revealed through the orientation of mechanosensitive hair cells relative to each other and to the body axes. In each neuromast, the receptor organ of the lateral line, hair bundles are arranged in a mirror-symmetrical fashion. Here we show that the establishment of mirror symmetry is preceded by rotational rearrangements between hair-cell pairs, a behavior consistently associated with the division of hair-cell precursors. Time-lapse imaging of *trilobite* mutants, which lack the core PCP constituent Vang-like protein 2 (Vangl2), shows that their misoriented hair cells correlate with misaligned divisions of hair-cell precursors and an inability to complete rearrangements accurately. Vangl2 is asymmetrically localized in the cells of the neuromast, a configuration required for accurate completion of rearrangements. Manipulation of Vangl2 expression or of Notch signaling results in a uniform hair-cell polarity, indicating that rearrangements refine neuromast polarity with respect to the body axes.

Key words: Neurogenin, Notch, Planar cell polarity, Vang-like protein 2

Introduction

PCP is established through a complex signaling network comprising evolutionarily conserved core components and their tissue-specific effectors (Goodrich and Strutt, 2011). Although the asymmetric subcellular localization of PCP components ensures the directional propagation of polarity signals, it remains unclear how asymmetry is established initially and how cells interpret polarity information (Wu and Mlodzik, 2009; Aigouy et al., 2010).

A sensory organ that detects water displacement, the neuromast consists of a cluster of mechanosensitive hair cells separated by nonsensory supporting cells and surrounded by mantle cells (Metcalfe, 1985; Ghysen and Dambly-Chaudière, 2007; Hernández et al., 2007). Hair cells of the zebrafish's lateral line are morphologically and functionally similar to those of the inner ear. Originating in pairs from oriented division of precursors (López-Schier and Hudspeth, 2006; Wibowo et al., 2011), hair cells assume mirror symmetry, each with its kinocilium oriented toward its sister cell (Rouse and Pickles, 1991; Ghysen and Dambly-Chaudière, 2007). The systematic production of oppositely oriented hair cells ensures the presence in each neuromast of a roughly equal number of cells responsive to stimuli in either direction along the neuromast's axis of sensitivity.

How mirror symmetry arises in lateral line neuromasts is not known. We have therefore inquired how planar polarity is established and how axial information is interpreted by differentiating hair cells during development and regeneration.

Materials and Methods

Zebrafish strains and transgenic lines

Zebrafish (*Danio rerio*) were maintained by standard procedures (Westerfield, 2000).

The following mutant and transgenic lines were used: *vangl2/trilobite*, tri^{m209} (Jessen et al., 2002), *neurogenin1,* $ngn1^{hi059Tg}$ (ZIRC), *ET4*, $Et(krt4:GFP)^{sqet4}$ (Parinov et al., 2004), and *cldnB:lynGFP*, *Tg(-8.0cldnb:lynEGFP)* (Haas and Gilmour, 2006). The $Tg(myosin6b:mCherry^{CAAX})$ and *Tg(myosin6b:RFP-Vangl2)* lines were generated through standard Tol2-mediated transposition techniques (Kwan et al., 2007).

Cloning and mRNA production

For generation of a 5′ entry clone containing the *myosin6b* promoter (Obholzer et al., 2008) we produced by PCR a linear fragment with flanking HindIII and ClaI sites and ligated it into the unique sites of p5E-MCS. For the generation of entry clones containing TagRFP (Evrogen, Moscow, Russia), *Xenopus centrin 1* (pCS2-EGFP-Xcentrin), and *vangl2* (Addgene plasmid 17067; Addgene, Cambridge, MA), sequences were amplified by PCR with primers containing appropriate *att* sites (Kwan et al., 2007).

TagRFP:

5′ GGGGACAAGTTTGTACAAAAAAGCAGGCTGGACCATGGTGTCTA-AGGGCGA 3′

5′ GGGGACCACTTTGTACAAGAAAGCTGGATTAAGTTTGTGCCCCAG-TTTGCT 3′

Xenopus centrin:

5′ GGGGACAGCTTTCTTGTACAAAGTGGTTATGGCTTCTAACTACAA-GAAAC 3′

5′ GGGGACAACTTTGTATAATAAAGTTGGTCAGAATAAACTTGTCTT-CTTCAT 3′

vangl2:

5′ GGGGACAGCTTTCTTGTACAAAGTGGGGATGGATAACGAGTCGC-AGTACTCAG 3′

5′ GGGGACAACTTTGTATAATAAAGTTGGTCACACCGAGGTTTCCGACTGGAGCCG 3′

For the generation of the middle entry clone containing TagRFP, the Kozak sequence CTGGACC was inserted between the *attB1* site and the start codon.

RFP-Xcen mRNA was synthesized with the mMessage mMachine kit (Ambion, Austin, TX). Approximately 200 pg of mRNA was injected into each single-cell embryo.

Cell labeling and analysis of hair-cell orientation

Phalloidin staining and analysis of hair-cell orientation were performed as described (López-Schier et al., 2004). Neuromasts having eight or more mature hair cells were analyzed and those in which at least 70% of the hair cells exhibited a particular orientation were scored as biased. Neuromasts with defects in epithelial integrity and those with randomized orientations of hair cells were not scored.

The subcellular localization of RFP-Vangl2 was analyzed in Z-stack images of living *myo6b:RFP-Vangl2;cldnb:lynGFP* larvae. The orientations of hair cells in *myo6b:RFP-Vangl2* lines were analyzed either in Z-stack images of living *myo6b:RFP-Vangl2;cldnb:lynGFP* larvae or in fixed, phalloidin-stained samples from the incross of *myo6b:RFP-Vangl2* fish. The fluorescence of RFP was not detectable in fixed samples. For analysis of the Vangl2 overexpression phenotype in fixed samples, larvae with the highest level of RFP-Vangl2 expression were selected from the incross and processed for phalloidin staining.

DAPT treatment and hair-cell ablation

N-[*N*-(3,5-difluorophenacetyl-L-alanyl)]-*S*-phenylglycine *t*-butyl ester (DAPT; EMD Chemicals, Gibbstown, NJ) was solubilized in dimethyl sulfoxide and added to E3 medium at a final concentration of 10–100 μM. Fish were maintained in DAPT solutions at room temperature. To exclude effects of the solubilization vehicle, control larvae were also raised in 1% dimethyl sulfoxide. For recovery experiments, the DAPT solution was replaced after 2 d of treatment with fish water supplemented with 3 μM methylene blue and the animals were left to develop for several days before fixation.

For time-lapse imaging of *cldnB:lynGFP;myosin6b:mCherry* larvae treated with DAPT, embryos at 3 dpf were placed in 50 μM DAPT solution in E3 medium for approximately 6 hr and the solution was replaced during imaging with 100 μM DAPT in E3 medium. *ngn1;cldnB:lynGFP* larvae at 4 dpf were incubated and imaged in a 50 μM solution of DAPT.

Because the sensitivity of neuromasts to DAPT decreases with age (Takebayashi et al., 2007; Ma et al., 2008), ablation of mature hair cells was induced prior to DAPT treatment to study its effect on regeneration in larvae older than 3 dpf. Because neuromasts are less sensitive to neomycin before 5 dpf, hair-cell ablation was induced by treatment with 5 μM $CuSO_4$ (Sigma, St. Louis, MO) in E3 medium for 1 hr at room temperature (Hernández et al., 2006; Ma et al., 2008). Regeneration of lateral line hair cells in 3 dpf larvae following $CuSO_4$ treatment has been described previously (Hernández et al., 2007; Nagiel et al., 2008).

Imaging and analysis of hair-cell rearrangements

Images of fixed samples were obtained as Z-stacks with a laser-scanning confocal microscope (Fluoview FV1000, Olympus America, Center Valley, PA). For time-lapse recordings, animals were anesthetized in 380 μM ethyl 3-aminobenzoate methanesulfonate (Tricaine, Sigma) and immobilized in 1% low-melting-point agarose in E3 medium. For each experimental condition three or four animals were mounted together and one or two neuromasts per animal were imaged in rapid succession with an automatic stage positioner. Neuromasts containing one to three pairs of mature hair cells were selected for time-lapse recordings. Samples were imaged through a 63 × /NA1.4 or 100 × /NA1.4 oil-immersion objective lens on an inverted microscope (Axiovert 200, Carl Zeiss Microscopy, Thornwood, NY) with a spinning-disk confocal system (Ultraview, Perkin-Elmer, Waltham, MA) and a charge-coupled-device camera (iXon EM, Andor, Belfast, UK). Z-stacks were collected at intervals of 3–10 min. Image stacks of *myosin6b:RFP-Vang2;cldnb:lynGFP* neuromasts were captured with a charge-coupled-device camera (Orca-ER, Hamamatsu Life Technologies, Gaitherburg, MD). All images were processed with ImageJ (National Institutes of Health, Bethesda, MD) or Metamorph software (Molecular Devices, Sunnyvale, CA).

Results

Rearrangements of immature hair-cell pairs follow precursor divisions

The hair cells within each neuromast are aligned relative to their neighbors and to the anteroposterior and dorsoventral body axes (Fig. 1A). The planar orientation of the hair cells within a neuromast is thought to be determined by the direction of primordium migration (López-Schier et al., 2004). The first three branches of the posterior lateral line are formed by the rostral-caudal migration of three distinct primordia during the first week of development (Ghysen and Dambly-Chaudière, 2007). Neuromasts deposited by the first primordium are sensitive along the anteroposterior axis, whereas those deposited by the second primordium and its dorsal branch migrate ventrally after deposition and exhibit dorsoventral sensitivity (supplementary material Fig. S1) (López-Schier et al., 2004; Nuñez et al., 2009).

Our time-lapse imaging confirmed that most early divisions of hair-cell precursors in an anteroposteriorly sensitive neuromast occur near the dorsal or ventral pole (López-Schier and Hudspeth, 2006; Wibowo et al., 2011). Seventy percent of 23 divisions of hair-cell precursors lay along the axis of PCP (Fig. 1B,C). Approximately 40 min after the conclusion of cytokinesis, the daughter cells underwent stereotypical rearrangements (Wibowo et al., 2011) in which the two rotated about an axis through their interface (Fig. 1D,E; supplementary material Movies 1, 2). To distinguish immature hair cells from supporting cells, we created a transgenic line expressing membrane-bound mCherry under the control the hair cell-specific promoter *myosin6b* (Kwan et al., 2007; Obholzer et al., 2008). Imaging of neuromasts in *cldnB:lynGFP;myo6b:mCherry*^{CAAX} larvae showed that the promoter is active at low levels even before the onset of rearrangements (Fig. 1D,E). The initiation of rearrangements coincided with the acquisition of a typical “bottle” shape by the differentiating hair cells before their narrow apical parts had formed (Fig. 1F; supplementary material Movie 2). The completion of rearrangements was followed by vertical alignment of the hair cells’ apical parts, formation of the cuticular plates, asymmetric positioning of the kinocilia, and maturation of the hair bundles.

In 71% of the 24 rearrangements examined, the daughter hair cells reversed positions along the axis of PCP (Fig. 1D–F). Regardless of their positions within the neuromast, the remaining hair-cell pairs also initiated rearrangements but eventually returned to their original configurations. Either reversal or maintenance of the original positions resulted in a mirror-symmetrical polarization of the resultant hair cells.

Because PCP signaling underlies the asymmetric positioning of the primary cilium in some embryonic organs (Gray et al., 2011), we initiated our study of the establishment of mirror symmetry by tracing the events leading to ciliogenesis. Following the centrosomal component centrin revealed that alignment of the division axis was preceded by the rotation of centrosomal pairs (Fig. 2A; supplementary material Movie 1) and that the initiation of cellular rearrangements coincided with the apical movement of centrosomes (Fig. 2B). The axes of 30% of the divisions were perpendicular or oblique to the axis of PCP; in these instances the rearrangement was followed by an additional rotation of the immature hair-cell pair to achieve alignment with the PCP axis (Fig. 2B). Regardless of the axis of PCP, supporting-cell precursors divided radially with respect to a neuromast’s center. The apical translocation of centrosomes in immature supporting cells was not followed by rearrangements or active movements (Fig. 2C). These observations suggest that a mechanism intrinsic to immature hair-cell pairs establishes mirror symmetry.

Vangl2 mutants display defects in the accuracy of rearrangements

Van Gogh in *Drosophila* and its ortholog Vang-like protein 2 (Vangl2) in vertebrates are components of the core PCP signaling

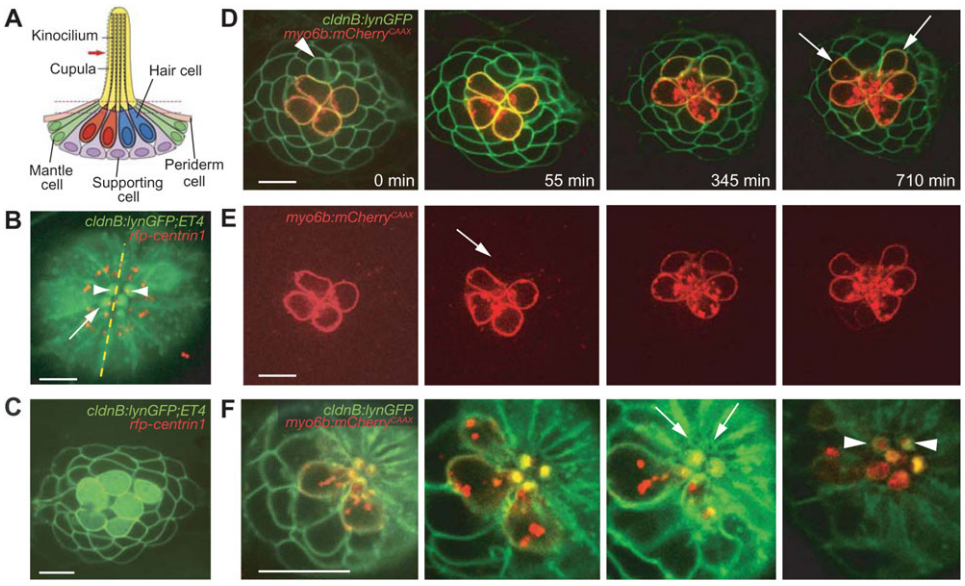

Fig. 1. Rearrangements by pairs of newly formed hair cells. (**A**) In a schematic depiction of a neuromast, four mechanoreceptive hair cells are surrounded by nonsensory supporting, mantle, and periderm cells. The asymmetric position of the kinocilium demarcates each hair cell's axis of planar polarity. (**B**) An apical view of a neuromast from a *cldnB:lynGFP;ET4* doubly transgenic fish shows green fluorescence in the plasma membranes of all cells and in the cytoplasm of only the hair cells. This projection of several sections through the neuromast's apex shows the actin-rich cuticular plates of hair cells (arrow). RFP-tagged centrin (red) labels centrosomes and indicates the orientation of each hair cell by marking the position of its kinociliary basal body (arrowheads). The neuromast's plane of mirror symmetry is designated by the dotted line. In this and all subsequent figures the anterior direction is to the left and dorsal is upward. (**C**) In an image from a single plane in the same preparation, supporting cells and hair-cell precursors express only membrane-associated GFP and are morphologically indistinguishable. Cytoplasmic GFP demarcates the mature hair cells. (**D**) A time-lapse series focussed at or above the level of hair-cell nuclei documents the rearrangement of a pair of immature hair cells (arrowhead) in a *cldnB:lynGFP;myo6b:mCherry*^{CAAX} larva. Rearrangements are specific to the daughter hair cells arising from a recent division and result in the mirror-symmetrical orientation of the pair. After completing their rearrangement, the maturing cells assume their final shapes (arrows). (**E**) The red channel of the foregoing time-lapse series visually isolates mature hair cells labeled with membrane-associated mCherry. Note the low level of labeling (arrow) in the newborn pair undergoing rearrangement. (**F**) The narrow apices of the immature pair of hair cells can first be observed in the third panel (arrows). As the apical membranes expand to encompass hair bundles, the orientations of the newly formed pair (arrowheads) can be determined from the positions of the openings in their cuticular plates. The scale bars represent 10 μm in all panels.

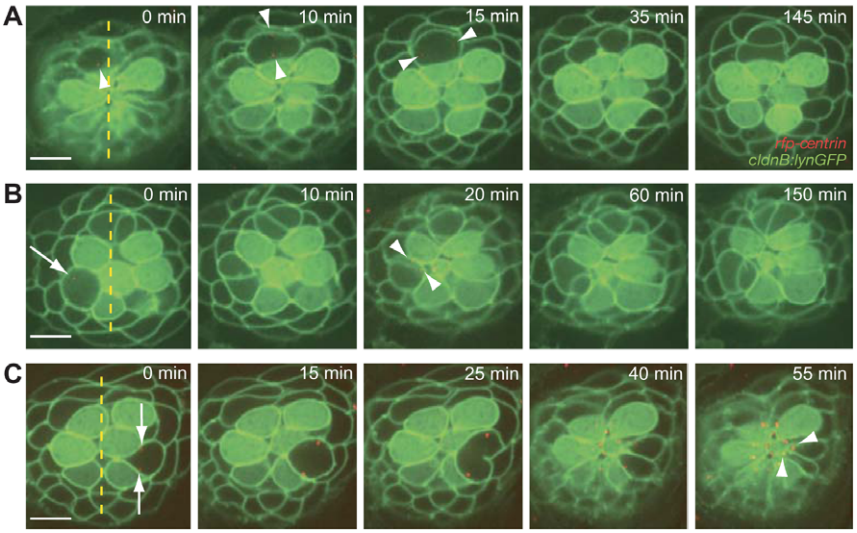

Fig. 2. Normal cellular positioning and orientation in a neuromast. (**A**) The centrosomes of a dividing hair-cell precursor, which are marked red with centrin-RFP (arrowheads), rotate 90° to position the axis of division along the neuromast's axis of polarity. After cytokinesis has been completed, rearrangement between the daughter cells commences. (**B**) A time-lapse series shows the rearrangement of a pair of hair cells following the division of a precursor orthogonally to a neuromast's axis of polarity. An arrow in the first panel marks the position of one centrosome in a dividing hair-cell precursor; the other centrosome is out of the plane of focus. Apical movement of the centrosomes (arrowheads) coincides with the rearrangement, after which the hair-cell pair undergoes an additional 90° rotation to align with the neuromast's axis of polarity. Note the rearrangement of a second pair of nascent hair cells at the dorsal pole of the neuromast. (**C**) A pair of supporting cells is formed through the symmetric division of a precursor positioned laterally to the central cluster of hair cells. The centrosomes in the precursor (arrows) move to position the axis of division obliquely relative to the neuromast's axis of planar polarity. Although the centrosomes move apically (arrowheads), the supporting-cell pair does not undergo rearrangements. The scale bars represent 10 μm in all panels.

pathway (Wolff and Rubin, 1998; Jessen et al., 2002; Montcouquiol et al., 2003). Mutations in *vangl2* cause misorientation of hair cells in the mammalian inner ear and in zebrafish neuromasts (Montcouquiol et al., 2003; López-Schier and Hudspeth, 2006). Time-lapse imaging of *trilobite* larvae showed that 12 of 16 hair-cell rearrangements did not result in complete reversals of position (Fig. 3A–D; supplementary material Movie 3). Moreover, cellular rearrangements in *trilobite* larvae lasted more than twice as long as those of wild-type animals and showed greater variability (Fig. 3E). We also observed multiple reversals that contributed to the increase and variability in duration for *trilobite* larvae (supplementary material Movie 4). The hair-cell precursors of mutants frequently appeared in the anterior or posterior regions of anteroposteriorly oriented neuromasts, whereas those of wild-type animals remained near the midline of the organ (Fig. 3A). Although the first two or three hair-cell pairs in *trilobite* neuromasts were usually aligned with the normal axis of PCP, nearly half of the subsequent divisions occurred at 45°–90° to that axis (Fig. 3A,F). In one instance the division was aligned with the axis of PCP, but after rearrangements the hair cells lay perpendicular to that correct orientation. These defects suggest that immature hair cells deficient in Vangl2 are unable to detect positional information or to rotate consistently.

DAPT treatment affects the establishment of mirror symmetry

Notch-Delta signaling is involved in the differentiation of hair cells (Brooker et al., 2006; Ma and Raible, 2009) and downregulation of the pathway results in formation of supernumerary hair cells. Ommatidia in the *Drosophila* eye likewise develop mirror symmetry through the interaction of PCP signaling with the Notch pathway (Fanto and McNeill, 2004). We therefore examined the possible role of the Notch pathway in hair-cell rearrangements by exposing 2 dpf embryos to the γ-secretase inhibitor DAPT, an inhibitor of Notch signaling (Geling et al., 2002). This treatment, which like mutations that affect Notch signaling does not affect neuromast deposition (Itoh and Chitnis, 2001; Lecaudey et al., 2008), yielded large neuromasts with excess hair cells of randomized orientations. Neuromasts frequently had irregular, concave shapes, perhaps resulting from the depletion of basally located supporting cells.

The hair cells in some neuromasts affected by DAPT showed a non-random orientation along the anteroposterior or dorsoventral axis. The anteroposteriorly oriented neuromasts derived from the first primordium displayed a clear bias toward an anterior orientation of hair cells (Fig. 4A,B; supplementary material Table S1; supplementary material Fig. S1). When DAPT was removed after one or two days of incubation, the bias was

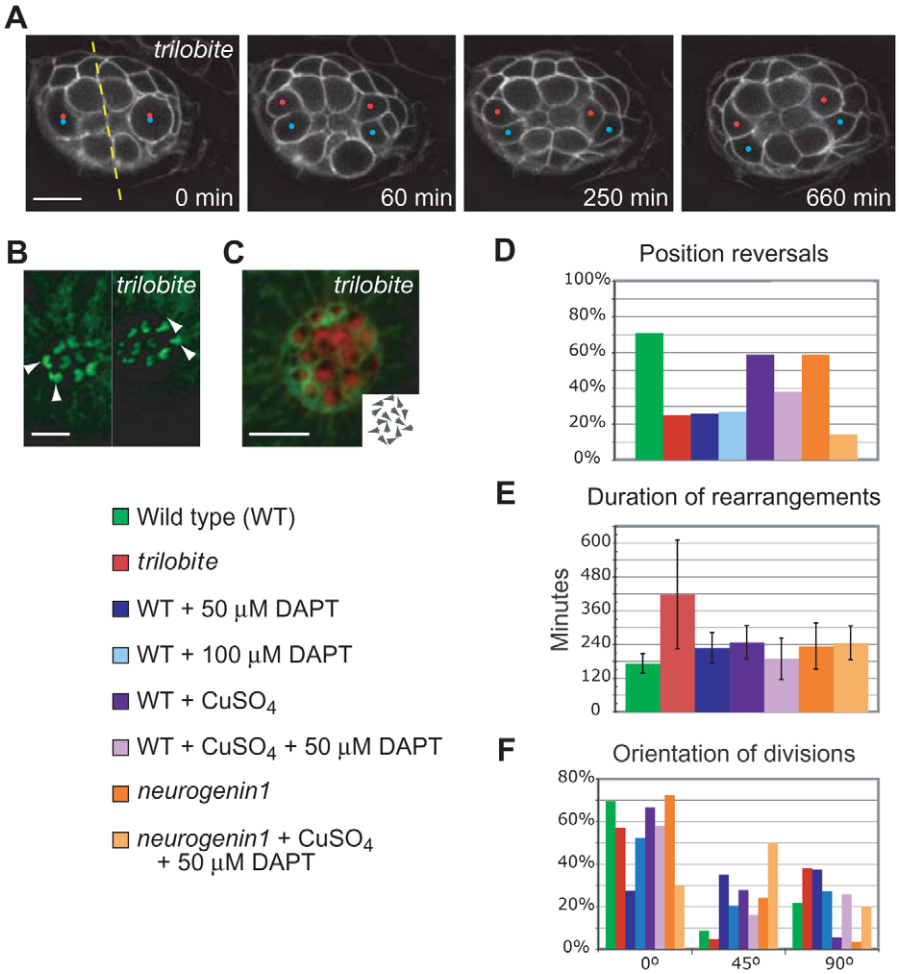

Fig. 3. Hair-bundle misorientation in *trilobite* mutants. (**A**) A time-lapse series of a neuromast from a *cldnB:lynGFP;tri* larva demonstrates that nascent hair cells have an impaired capacity to complete rearrangements. Two precursor divisions, each marked by a pair of dots, occur simultaneously at the lateral edges of the neuromast. The divisions occur perpendicularly to the neuromast's axis of polarity and parallel with its plane of mirror symmetry (dashed line). Although the daughter cells initiate rearrangements, they do not reverse positions. The scale bar represents 10 μm. (**B**) Micrographs of the cellular apices taken at the end of the same recording document the final orientations of the four newly formed hair cells (arrowheads). The scale bar represents 5 μm. (**C**) Phalloidin staining of a more mature neuromast shows the randomized orientation of mature hair cells in a *trilobite* mutant, which is schematized in the insert. The scale bar represents 5 μm. Panels **D**–**F** provide quantification of hair-cell rearrangements under different experimental conditions and with various genetic backgrounds. All larvae, including those in control experiments, were exposed to 1% dimethyl sulfoxide, the solubilization vehicle for DAPT. (D) The percentage of position reversals between pairs of nascent hair cells differs strongly between 22 wild-type neuromasts (green) and 15 *trilobite* organs (red). The other experimental conditions are described in the text. (E) The average time devoted to rearrangements is significantly greater for 15 *trilobite* larvae than for 22 wild-type animals ($p<0.01$). The duration of rearrangements in animals treated with 100 μM DAPT could not be accurately determined. (F) The orientation of divisions of hair-cell precursors relative to the neuromast's polarity axis shows the profound effect of the *trilobite* mutation.

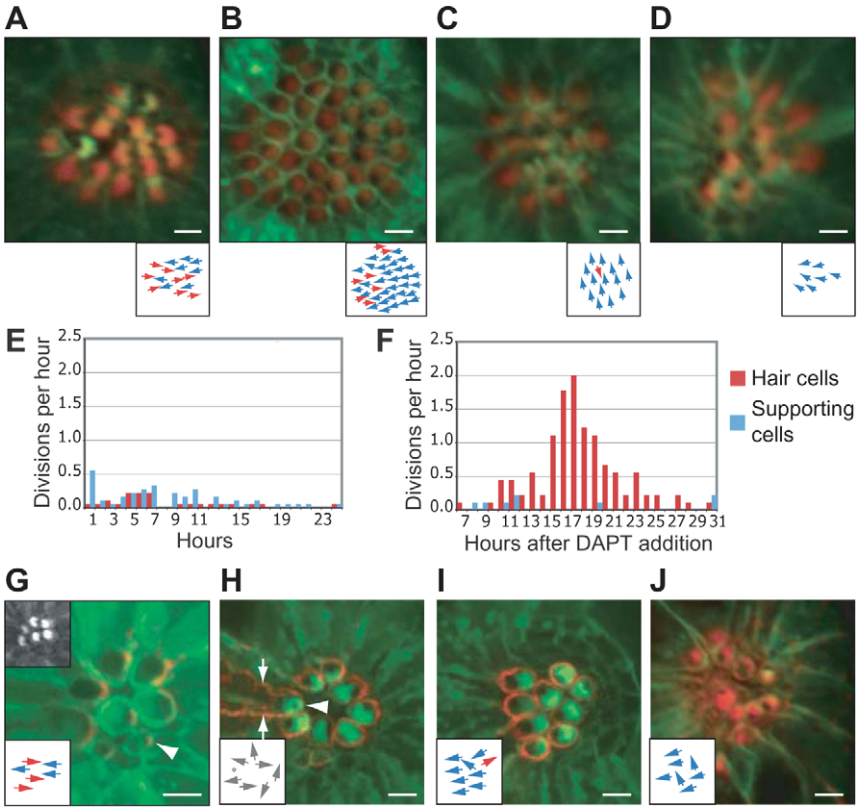

Fig. 4. Effects of DAPT treatment and loss of asymmetric Vangl2 localization. (**A**) Phalloidin staining (red) of a wild-type *cldnB:lynGFP* larva demonstrates the normal orientation of hair bundles in an anteroposteriorally polarized neuromast derived from the first primordium. This and the subsequent micrographs show apical views of neuromasts from *cldnB:lynGFP* larvae; the subjacent diagrams indicate the orientations of the hair cells. (**B**) The numerous hair cells in a neuromast of similar age treated with 100 µM DAPT display a strong bias toward an anterior orientation. (**C**) After exposure to 100 µM DAPT, the hair bundles in a neuromast derived from the second primordium show a striking dorsal bias. (**D**) A neuromast derived from the first primordium in a *neurogenin1* larva displays an anterior bias after exposure to only 50 µM DAPT. (**E**) Under control conditions, the production of hair cells (red) and supporting cells (blue) is relatively constant during an observation period beginning at 3 dpf. (**F**) In wild-type larvae a burst of hair-cell production begins 17–22 hr after the addition of 100 µM DAPT; the differentiation of supporting cells is meanwhile suppressed. Note that imaging commenced 7 hr after exposure to 100 µM DAPT. (**G**) In a neuromast of a *myo6b:RFP-Vangl2;cldnB:lynGFP* larva, Vangl2 (red) occurs in hair cells at the level of the apical actin belt surrounding the cuticular plate. An immature hair cell is labeled with an arrowhead. The top left inset shows the apices of the hair cells in the green channel. The lower inset in this and the subsequent illustrations schematizes the orientations of hair bundles. (**H**) Overexpression of Vangl2 eliminates the specific enrichment of the protein at the posterior apex and causes hair-cell misorientation. The mature hair cell with the strongest expression, which extends down the cell's lateral borders (arrows), has a centrally placed kinocilium (arrowhead; dot in the inset). (**I**) Another neuromast with high levels of Vangl2 expression (red) displays a bias toward anterior orientations. (**J**) A neuromast from a *cldnB:lynGFP;tri* larva treated with 50 µM DAPT and stained with phalloidin (red) contains hair cells with an anterior bias. The scale bars represent 10 µm in all panels.

particularly pronounced as neuromasts recovered through the replenishment of supporting cells.

DAPT affected hair-cell orientation in a time- and dosage-dependent manner. Because treatment earlier in development or a more posterior position of the neuromast increased the probability of a biased hair-cell orientation, developing neuromasts apparently have a higher sensitivity to DAPT. Greater concentrations of DAPT also raised the percentage of affected neuromasts (supplementary material Table S1). Although a bias toward posterior orientation was rare under all experimental conditions, a greater percentage of neuromasts showed that bias after exposure to high concentrations of DAPT (supplementary material Table S1). A bias in either direction usually occurred in two or more neuromasts in an animal; a combination of anteriorly and posteriorly biased neuromasts was never observed in the same animal. The neuromasts derived from the second primordium or its dorsal branch evinced strong biases toward respectively a dorsal or a ventral orientation (Fig. 4C; supplementary material Table S1). Early DAPT treatment also affected the global orientation of neuromasts; several displayed an almost complete transition from a dorsoventral to an anteroposterior orientation (supplementary material Fig. S2). Some neuromasts derived from the second primordium evinced a bias towards dorsal orientation or a transition to anteroposterior orientation. These neuromasts were nevertheless localized ventral to the first-primordium neuromasts, so the direction and extent of primordium migration are not affected by DAPT treatment.

Because each axon of the posterior lateral-line nerve preferentially innervates cells of a common polarity (Nagiel et al., 2008; Faucherre et al., 2009), we next asked whether nerve fibers act instructively in the rearrangement process. *neurogenin1* mutants lack both afferent axons and peripheral glia (Andermann et al., 2002; López-Schier and Hudspeth, 2005) but develop small, supernumerary neuromasts with normal hair-cell morphology, planar polarity, and capacity for regeneration (Nagiel et al., 2008). Because of the high sensitivity of *neurogenin1* mutants to DAPT, reflected in extensive mortality upon exposure to concentrations greater than 50 µM, we

subjected larvae at 4 dpf to 50 μM DAPT after Cu^{2+} treatment had triggered hair-cell regeneration. The treatment resulted in an anterior bias comparable to that in control fish treated earlier in development or with 100 μM DAPT (Fig. 4D; supplementary material Table S1). In untreated *neurogenin1* neuromasts hair-cell pairs underwent rearrangements, 59% of which yielded reversals (Fig. 3D). Like wild-type neuromasts treated with 100 μM DAPT, *neurogenin1* mutant neuromasts exposed to 50 μM DAPT manifested a significant decrease in the percentage of reversals. Because Neurogenin1 serves both as a transcriptional regulator and as a target of the Notch pathway (Ma et al., 1996; Blader et al., 1997; Madelaine and Blader, 2011), the increased sensitivity of the mutants supports the idea that the effects of DAPT on rearrangements reflect its effect on Notch signaling.

We next examined whether DAPT treatment affects the divisions of hair-cell precursors in developing neuromasts. Time-lapse imaging of developing wild-type neuromasts containing no more than six mature hair cells and treated at 3 dpf with 100 μM DAPT demonstrated that the supernumerary hair cells arose by division of unipotent precursors rather than by transdifferentiation of supporting cells (Fig. 4E,F; supplementary material Movie 5). During the mitotic peak following the addition of DAPT, almost all divisions yielded hair-cell pairs that initiated rearrangements. No rearrangements were observed between a hair cell and a supporting cell or between non-sibling hair cells. Nor did we observe expression of mCherry driven by the *myo6b* promoter in a single immature cell contacting the differentiated hair cells. This result suggests that defects in Notch-mediated lateral inhibition do not yield supernumerary hair cells. We conclude that DAPT treatment of developing neuromasts increases the division rate of hair-cell precursors but decreases the ability of hair-cell pairs to undergo reversals (Fig. 4E,F; supplementary material Fig. S3). Notch signaling evidently limits the proliferation of hair-cell precursors in developing neuromasts as it does in regenerating larval neuromasts (Ma et al., 2008).

Asymmetric localization of Vangl2 in hair-cell orientation

Because the asymmetric localization of core PCP factors is essential for the establishment of planar polarity (Goodrich and Strutt, 2011), we next examined the localization of Vangl2 in hair cells. Vang-like proteins localize asymmetrically in both hair cells and supporting cells of the vertebrate inner ear (Montcouquiol et al., 2006; Jones et al., 2008; Song et al., 2010; Warchol and Montcouquiol, 2010). Although the zebrafish *vangl2* transcript occurs in both cell types in lateral-line neuromasts (López-Schier and Hudspeth, 2006), the subcellular localization of the corresponding protein remains unknown. We therefore created transgenic lines of zebrafish expressing a RFP-Vangl2 fusion protein under the control of the *myosin6b* promoter. Vangl2 was greatly enriched at the level of the apical junctional complex (Fig. 4G-I). In neuromasts derived from the first primordium, RFP-Vangl2 was enriched asymmetrically at the caudal edges of both anteriorly and posteriorly oriented hair cells (Fig. 4G). The dorsoventrally oriented neuromasts derived from the second primordium showed enrichment at the ventral edges of hair cells. In both instances the uniformly asymmetric localization in all hair cells did not accord with the mirror symmetry of the neuromasts.

As observed in several independently derived transgenic lines, high levels of RFP-Vangl2 expression that abolished the protein's asymmetric distribution were associated with hair-cell misorientation resembling the *trilobite* phenotype (Fig. 4H; supplementary material Fig. S1). Because asymmetric localization could be observed only in live samples, we analyzed 84 neuromasts derived from the first primordium by live imaging of several RFP-Vangl2 transgenic lines. Normal hair-cell orientation was observed in 57 neuromasts; in 53 of these the correct planar polarity was associated with asymmetric localization of Vangl2 in hair cells (Fig. 4G). Twenty-seven of the 84 neuromasts displayed hair-cell misorientation, which in every case was associated with increased Vangl2 levels and the ubiquitous distribution of Vangl2 around the apical junctional complex (Fig. 4H,I). In six neuromasts that showed uniform apical accumulation we observed a bias toward an anterior orientation (Fig. 4I).

In order to investigate further the effect of Vangl2 overexpression, we analyzed hair-cell orientation in fixed samples from incrosses of transgenic carriers selected for high expression levels. In 16% of the 48 *myo6b:RFP-vangl2* neuromasts, overexpression resulted not in randomized orientation, but in hair cells showing an anterior bias. The loss of Vangl2 protein in combination with DAPT treatment occasionally yielded a similar phenotype. Although the neuromasts of *trilobite* larvae treated with 50 μM DAPT at 2 dpf rarely differentiated properly, patches of hair cells with an orientation bias were sometimes observed (Fig. 4J). These results suggest that the asymmetric localization of Vangl2 is required for proper hair-cell orientation but that another signal acts instructively in the establishment of mirror symmetry (Deans et al., 2007).

Discussion

The establishment of mirror symmetry represents an evolutionarily conserved mechanism for the regulation of tissue form and function. In several tissues with mirror symmetry, notably the vestibular sensory epithelia, cells are aligned across the epithelial plane through PCP signaling (Montcouquiol et al., 2003; Montcouquiol et al., 2006; Wang et al., 2006; Deans et al., 2007). Our study suggests that mirror symmetry in a developing neuromast arises from rotational rearrangements between immature pairs of hair cells, a phenomenon has not been observed in the murine vestibular system (Deans et al., 2007). Although oriented cell division does not yield mirror symmetry directly, we find that the division of a hair-cell precursor always precedes the cell rearrangements that establish the pattern. Following cytokinesis, each nascent pair of hair cells undergoes movements that result either in a reversal or in a return to the original position along a neuromast's axis of sensitivity. Rotation of the hair-cell pair as a unit follows the initial rearrangements when the axis of division is not already aligned with the neuromast's axis of sensitivity.

In the *trilobite* mutant a defect in PCP signaling results in misoriented hair cells. This phenotype is associated with frequent misalignments in the divisions of hair-cell progenitors, high variability in the duration of hair-cell rearrangements, and a failure to complete reversals accurately. All of these features support a role for Vangl2 in the interpretation of polarity information and the regulation of cytoskeletal organization.

To study events that are instructive for hair-cell rearrangements, we used chemical inhibitors to examine a candidate signaling pathway reversibly and with temporal precision. We found that treatment with DAPT, an inhibitor of the Notch pathway, disrupts the rearrangements and inhibits the reversal of immature hair cells. In *mindbomb* mutants, which experience a deficit in the Notch pathway, defects in lateral inhibition cause the differentiation of supernumerary hair cells in the inner ear at the expense of supporting cells (Haddon et al., 1998; Haddon et al., 1999; Itoh and Chitnis, 2001). In neuromasts regenerating after hair-cell ablation at 5 dpf, partial inhibition of Notch signaling with DAPT increases proliferation and the subsequent formation of excess hair cells (Ma et al., 2008). However, DAPT treatment without hair-cell ablation has no effect on hair-cell numbers at this stage. Examining the effects of high concentrations of DAPT on hair-cell numbers and rearrangements earlier in development, we observed an increase in the number of dividing hair-cell precursors without prior removal of mature hair cells. This effect may be attributed to the different cellular composition of recently deposited versus more mature neuromasts: in cultured fetal mouse cochleae, the pool of transient progenitors susceptible to DAPT treatment decreases over time (Takebayashi et al., 2007). Recently deposited neuromasts may likewise contain a high proportion of transient progenitors capable of proliferating upon DAPT treatment.

We unexpectedly found that DAPT treatment and overexpression of Vangl2 can cause hair cells within a neuromast to adopt an almost uniform alignment. The orientation bias appears to be correlated with an inability of rearranging hair-cell pairs to achieve stable reversals of position. This result and the observation that more than half of hair-cell pairs in both wild-type and *neurogenin1* larvae undergo reversals suggests that neuromasts display an intrinsic preference for a uniform orientation that is overridden by the rotation of hair cells relative to one another. This innate polarity is distinct for each of the three primordia and can be reversed independently of the direction of primordium migration. Our findings represent a basis for future attempts to characterize the long-range signals that instruct hair-cell reversals, maintenance of this underlying innate polarity, and the establishment of mirror symmetry.

Acknowledgements

The authors thank A. Afolalu and N. McKenney for fish husbandry; the late C. B. Chien, D. Gilmour, V. Korzh, K. Kwan, T. Nicolson, N. Obholzer, L. Solnica-Krezel, and ZIRC for zebrafish lines and reagents; A. North and M. Vologodskaia for technical assistance; and A. Steiner, J. Wu, and the members of our research group for comments on the manuscript. This investigation was supported by grant DC000241 from the National Institutes of Health. A. J. H. is an Investigator of Howard Hughes Medical Institute.

Competing Interests

The authors declare no competing financial interests.

References

Aigouy, B., Farhadifar, R., Staple, D. B., Sagner, A., Röper, J. C., Jülicher, F. and Eaton, S. (2010). Cell flow reorients the axis of planar polarity in the wing epithelium of Drosophila. *Cell* **142**, 773-786.

Andermann, P., Ungos, J. and Raible, D. W. (2002). Neurogenin1 defines zebrafish cranial sensory ganglia precursors. *Dev. Biol.* **251**, 45-58.

Blader, P., Fischer, N., Gradwohl, G., Guillemot, F. and Strähle, U. (1997). The activity of neurogenin1 is controlled by local cues in the zebrafish embryo. *Development* **124**, 4557-4569.

Brooker, R., Hozumi, K. and Lewis, J. (2006). Notch ligands with contrasting functions: Jagged1 and Delta1 in the mouse inner ear. *Development* **133**, 1277-1286.

Deans, M. R., Antic, D., Suyama, K., Scott, M. P., Axelrod, J. D. and Goodrich, L. V. (2007). Asymmetric distribution of prickle-like 2 reveals an early underlying polarization of vestibular sensory epithelia in the inner ear. *J. Neurosci.* **27**, 3139-3147.

Fanto, M. and McNeill, H. (2004). Planar polarity from flies to vertebrates. *J. Cell Sci.* **117**, 527-533.

Faucherre, A., Pujol-Martí, J., Kawakami, K. and López-Schier, H. (2009). Afferent neurons of the zebrafish lateral line are strict selectors of hair-cell orientation. *PLoS ONE* **4**, e4477.

Geling, A., Steiner, H., Willem, M., Bally-Cuif, L. and Haass, C. (2002). A gamma-secretase inhibitor blocks Notch signaling in vivo and causes a severe neurogenic phenotype in zebrafish. *EMBO Rep.* **3**, 688-694.

Ghysen, A. and Dambly-Chaudière, C. (2007). The lateral line microcosmos. *Genes Dev.* **21**, 2118-2130.

Goodrich, L. V. and Strutt, D. (2011). Principles of planar polarity in animal development. *Development* **138**, 1877-1892.

Gray, R. S., Roszko, I. and Solnica-Krezel, L. (2011). Planar cell polarity: coordinating morphogenetic cell behaviors with embryonic polarity. *Dev. Cell* **21**, 120-133.

Haas, P. and Gilmour, D. (2006). Chemokine signaling mediates self-organizing tissue migration in the zebrafish lateral line. *Dev. Cell* **10**, 673-680.

Haddon, C., Jiang, Y. J., Smithers, L. and Lewis, J. (1998). Delta-Notch signalling and the patterning of sensory cell differentiation in the zebrafish ear: evidence from the mind bomb mutant. *Development* **125**, 4637-4644.

Haddon, C., Mowbray, C., Whitfield, T., Jones, D., Gschmeissner, S. and Lewis, J. (1999). Hair cells without supporting cells: further studies in the ear of the zebrafish mind bomb mutant. *J. Neurocytol.* **28**, 837-850.

Hernández, P. P., Moreno, V., Olivari, F. A. and Allende, M. L. (2006). Sub-lethal concentrations of waterborne copper are toxic to lateral line neuromasts in zebrafish (Danio rerio). *Hear. Res.* **213**, 1-10.

Hernández, P. P., Olivari, F. A., Sarrazin, A. F., Sandoval, P. C. and Allende, M. L. (2007). Regeneration in zebrafish lateral line neuromasts: expression of the neural progenitor cell marker sox2 and proliferation-dependent and-independent mechanisms of hair cell renewal. *Dev. Neurobiol.* **67**, 637-654.

Itoh, M. and Chitnis, A. B. (2001). Expression of proneural and neurogenic genes in the zebrafish lateral line primordium correlates with selection of hair cell fate in neuromasts. *Mech. Dev.* **102**, 263-266.

Jessen, J. R., Topczewski, J., Bingham, S., Sepich, D. S., Marlow, F., Chandrasekhar, A. and Solnica-Krezel, L. (2002). Zebrafish trilobite identifies new roles for Strabismus in gastrulation and neuronal movements. *Nat. Cell Biol.* **4**, 610-615.

Jones, C., Roper, V. C., Foucher, I., Qian, D., Banizs, B., Petit, C., Yoder, B. K. and Chen, P. (2008). Ciliary proteins link basal body polarization to planar cell polarity regulation. *Nat. Genet.* **40**, 69-77.

Kwan, K. M., Fujimoto, E., Grabher, C., Mangum, B. D., Hardy, M. E., Campbell, D. S., Parant, J. M., Yost, H. J., Kanki, J. P. and Chien, C. B. (2007). The Tol2kit: a multisite gateway-based construction kit for Tol2 transposon transgenesis constructs. *Dev. Dyn.* **236**, 3088-3099.

Lecaudey, V., Cakan-Akdogan, G., Norton, W. H. and Gilmour, D. (2008). Dynamic Fgf signaling couples morphogenesis and migration in the zebrafish lateral line primordium. *Development* **135**, 2695-2705.

López-Schier, H. and Hudspeth, A. J. (2005). Supernumerary neuromasts in the posterior lateral line of zebrafish lacking peripheral glia. *Proc. Natl. Acad. Sci. USA* **102**, 1496-1501.

López-Schier, H. and Hudspeth, A. J. (2006). A two-step mechanism underlies the planar polarization of regenerating sensory hair cells. *Proc. Natl. Acad. Sci. USA* **103**, 18615-18620.

López-Schier, H., Starr, C. J., Kappler, J. A., Kollmar, R. and Hudspeth, A. J. (2004). Directional cell migration establishes the axes of planar polarity in the posterior lateral-line organ of the zebrafish. *Dev. Cell* **7**, 401-412.

Ma, E. Y. and Raible, D. W. (2009). Signaling pathways regulating zebrafish lateral line development. *Curr. Biol.* **19**, R381-R386.

Ma, E. Y., Rubel, E. W. and Raible, D. W. (2008). Notch signaling regulates the extent of hair cell regeneration in the zebrafish lateral line. *J. Neurosci.* **28**, 2261-2273.

Ma, Q., Kintner, C. and Anderson, D. J. (1996). Identification of neurogenin, a vertebrate neuronal determination gene. *Cell* **87**, 43-52.

Madelaine, R. and Blader, P. (2011). A cluster of non-redundant Ngn1 binding sites is required for regulation of deltaA expression in zebrafish. *Dev. Biol.* **350**, 198-207.

Metcalfe, W. K. (1985). Sensory neuron growth cones comigrate with posterior lateral line primordial cells in zebrafish. *J. Comp. Neurol.* **238**, 218-224.

Montcouquiol, M., Rachel, R. A., Lanford, P. J., Copeland, N. G., Jenkins, N. A. and Kelley, M. W. (2003). Identification of Vangl2 and Scrb1 as planar polarity genes in mammals. *Nature* **423**, 173-177.

Montcouquiol, M., Sans, N., Huss, D., Kach, J., Dickman, J. D., Forge, A., Rachel, R. A., Copeland, N. G., Jenkins, N. A., Bogani, D. et al. (2006). Asymmetric localization of Vangl2 and Fz3 indicate novel mechanisms for planar cell polarity in mammals. *J. Neurosci.* **26**, 5265-5275.

Nagiel, A., Andor-Ardó, D. and Hudspeth, A. J. (2008). Specificity of afferent synapses onto plane-polarized hair cells in the posterior lateral line of the zebrafish. *J. Neurosci.* **28**, 8442-8453.

Nuñez, V. A., Sarrazin, A. F., Cubedo, N., Allende, M. L., Dambly-Chaudière, C. and Ghysen, A. (2009). Postembryonic development of the posterior lateral line in the zebrafish. *Evol. Dev.* **11**, 391-404.

Obholzer, N., Wolfson, S., Trapani, J. G., Mo, W., Nechiporuk, A., Busch-Nentwich, E., Seiler, C., Sidi, S., Söllner, C., Duncan, R. N. et al. (2008). Vesicular glutamate transporter 3 is required for synaptic transmission in zebrafish hair cells. *J. Neurosci.* **28**, 2110-2118.

Parinov, S., Kondrichin, I., Korzh, V. and Emelyanov, A. (2004). Tol2 transposon-mediated enhancer trap to identify developmentally regulated zebrafish genes in vivo. *Dev. Dyn.* **231**, 449-459.

Rouse, G. W. and Pickles, J. O. (1991). Paired development of hair cells in neuromasts of the teleost lateral line. *Proc. Biol. Sci.* **246**, 123-128.

Song, H., Hu, J., Chen, W., Elliott, G., Andre, P., Gao, B. and Yang, Y. (2010). Planar cell polarity breaks bilateral symmetry by controlling ciliary positioning. *Nature* **466**, 378-382.

Takebayashi, S., Yamamoto, N., Yabe, D., Fukuda, H., Kojima, K., Ito, J. and Honjo, T. (2007). Multiple roles of Notch signaling in cochlear development. *Dev. Biol.* **307**, 165-178.

Wang, Y., Guo, N. and Nathans, J. (2006). The role of Frizzled3 and Frizzled6 in neural tube closure and in the planar polarity of inner-ear sensory hair cells. *J. Neurosci.* **26**, 2147-2156.

Warchol, M. E. and Montcouquiol, M. (2010). Maintained expression of the planar cell polarity molecule Vangl2 and reformation of hair cell orientation in the regenerating inner ear. *J. Assoc. Res. Otolaryngol.* **11**, 395-406.

Westerfield, M. (2000). *The Zebrafish Book: A Guide For The Laboratory Use Of Zebrafish (Danio Rerio)*, 4th edn. Eugene, OR, USA: University of Oregon Press.

Wibowo, I., Pinto-Teixeira, F., Satou, C., Higashijima, S. and López-Schier, H. (2011). Compartmentalized Notch signaling sustains epithelial mirror symmetry. *Development* **138**, 1143-1152.

Wolff, T. and Rubin, G. M. (1998). Strabismus, a novel gene that regulates tissue polarity and cell fate decisions in Drosophila. *Development* **125**, 1149-1159.

Wu, J. and Mlodzik, M. (2009). A quest for the mechanism regulating global planar cell polarity of tissues. *Trends Cell Biol.* **19**, 295-305.